Liquid Crystals
Publication details, including instructions for authors and subscription information:
http://www.informaworld.com/smpp/title~content=t713926090

An AC electro-optic technique of comparing the two anchoring energies of a hybrid aligned nematic cell

P. Maheswara Murthy[a]; V. A. Raghunathan[a]; N. V. Madhusudana[a]
[a] Raman Research Institute, Bangalore, India

To cite this Article Murthy, P. Maheswara , Raghunathan, V. A. and Madhusudana, N. V.(1993) 'An AC electro-optic technique of comparing the two anchoring energies of a hybrid aligned nematic cell', Liquid Crystals, 14: 4, 1107 — 1124
To link to this Article: DOI: 10.1080/02678299308027819
URL: http://dx.doi.org/10.1080/02678299308027819

LIQUID CRYSTALS, 1993, VOL. 14, NO. 4, 1107–1124

An AC electro-optic technique of comparing the two anchoring energies of a hybrid aligned nematic cell

by P. R. MAHESWARA MURTHY, V. A. RAGHUNATHAN and N. V. MADHUSUDANA*

Raman Research Institute, Bangalore 560080, India

We have found that the AC electro-optic response of a hybrid aligned nematic cell at the frequency (f) of an electric field applied normal to the plates can be conveniently used to compare the anchoring energies at the two surfaces. The f signal arises from the flexoelectric contribution to the surface torques when the anchoring energies are weak. For CCH-7, we have found by measurement of the optical path difference that the homeotropic alignment produced by a silane treatment has a weak anchoring energy. In this case, the f signal produced by an applied AC field exhibits a maximum and then a minimum as a function of the field. The reduction in the signal level after the maximum is caused by a lowering of the tilt angle at the surface treated for homeotropic alignment at high fields. The subsequent increase is caused by an effective weakening of the anchoring energy at the homogeneously aligned surface because of a sharp curvature distortion close to that surface. We have also found that the anchoring energy for homogeneous alignment of PCH-7 on an obliquely coated SiO plate is comparable to that at the homeotropically aligned surface.

1. Introduction

The alignment of a nematic liquid crystal on glass surfaces can be controlled by an appropriate treatment. In general, the director can make a tilt angle θ_0 with the normal to the surface of the plate. If $\theta_0 = 0$, the alignment is homeotropic and if $\theta_0 = \pi/2$, it is homogeneous. The anchoring energy refers to the strength of the anisotropic interaction between the nematic director and the substrate, and obviously depends on both the chemical nature of the liquid crystal and that of the substrate. The surface energy density is usually taken to be of the form $W/2 \sin^2 \theta_s$, where W is the anchoring energy, and θ_s is the tilt angle measured from the easy axis. This form takes into account the apolar nature of the nematic director. As the anchoring strength W increases, the energy density increases more steeply with θ_s from its minimum value at $\theta_s = 0$. Similar arguments hold for the anchoring energy for the azimuthal orientation ϕ. In the present paper we confine our attention to the tilt alignment θ.

It is obviously of considerable interest to measure W for different systems. In both liquid crystal displays and in the Fréedericksz transition technique of measuring the curvature elastic constants, we require a *strong* anchoring. A convenient measure of the inverse anchoring strength is given by the extrapolation length $L = K/W$ [1], where K is an appropriate elastic constant. If $L \ll d$, the sample thickness, which is usually the length over which a curvature deformation is produced, the anchoring is considered to be strong. If $L \sim d$, it is quite weak. There have been several attempts to measure W [2–7]. In general, the tilt angle at the surface takes an equilibrium value which balances the torque arising from the surface energy with that due to the curvature from the distortion of the director in the bulk. The latter distortion can be influenced either

* Author for correspondence.

0267–8292/93 $10·00

by the alignment of the director at another surface or by external orienting fields. In some studies, a destabilizing magnetic field $H \gg H_c$, where H_c is the Fréedericksz threshold, has been used for this purpose [2]. Similar measurements have also been made with applied electric fields [3, 4]. In these studies, it was found that W decreases with increase of temperature approximately as S^2, where S is the orientational order parameter. Further, it was also found that when the deviation angle θ_s is not very small, the simple $\sin^2 \theta_s$ form of the anchoring energy may not be adequate. W has also been measured for hybrid aligned cells in which one surface is treated for homeotropic alignment and the other for homogeneous alignment. If one of the surfaces has a *strong* anchoring., it produces a finite deviation angle θ_s at the other surface with weak anchoring [5, 7, 8]. If the thickness of the sample is reduced, θ_s increases and below a critical thickness, a uniformly aligned sample with the orientation dictated by the strongly anchored surface is obtained [5, 8]. In all these experiments, either an optical or a capacitance measurement is used to probe the director profile. If the anchoring energy is weak and the sample is subjected to an electric field, the surface torque has an additional contribution from the flexoelectric energy. As is well known, the flexoelectric energy density is a linear function of the curvature and hence does not give rise to bulk torque densities except through a non-uniform electric field which may arise from the dielectric anisotropy of the sample. On the other hand, if the surface anchoring is weak, it can change the distortion angle θ_s at the surface. This effect can be clearly seen under a DC field [9]. Since the flexoelectric contribution sensitively depends on weak anchoring, it is naturally a very useful probe of the anchoring energy. In the present work, we have used an applied AC electric field to probe the anchoring energy at *both* the surfaces of a hybrid aligned cell using the flexoelectric effect. This is done by monitoring the AC optical signal at the frequency f of the applied voltage. The f signal arises from the flexoelectric effect, in view of the linear dependence of the relevant energy density on E, the electric field. We have chosen materials with positive dielectric anisotropy $\Delta\varepsilon$ to avoid electrohydrodynamic instabilities which arise when $\Delta\varepsilon < 0$. The director profile in the bulk strongly depends on the applied root mean square field due to the dielectric coupling. At higher fields, the director tends towards homeotropic alignment. When the tilt angle on the surface is not equal to 0 or $\pi/2$, the flexoelectric contribution to the surface torque is non-zero and produces an f signal. Thus at high fields, the signal arises mainly from the oscillations of the director near the homogeneously aligned surface. We also present a simplified theoretical analysis of the problem.

2. Experimental technique and results

The nematic sample was mounted between two coated glass ITO plates. The upper plate was either treated with a polyimide and undirectionally rubbed or vacuum coated with silicon monoxide at an oblique angle to get a homogeneous alignment. The lower plate was treated to get a homeotropic alignment. The spacing of the empty cell d was measured using channel spectroscopy and was usually around 10 μm. The sample was placed on the stage of a Leitz polarizing microscope such that the plane in which the director is aligned makes an angle of 45° with the crossed polarizers. The temperature of the sample was controlled by using a Mettler FP 82 hot stage. The sample was illuminated with a helium–neon laser beam of low intensity. The transmitted light beam was monitored using a photo-diode. An electric field was applied to the sample and the output of the photo-diode was connected both to a Keithley nano-voltmeter (Model 181) and to a lock-in-amplifier (PAR Model 5301A) to measure both the DC

and AC components of the optical signal. A block diagram of the experimental set up is shown in figure 1. We also measured the optical path difference of the cell at zero field using a Leitz tilting compensator. The experiments were conducted on the following compounds obtained from commercial sources:

(*a*) *trans*-1-heptyl-4-(4-cyanocyclohexyl)cyclohexane (CCH-7), and
(*b*) *trans*-1-heptyl-4-(4-cyanophenyl)cyclohexane (PCH-7).

The optical path difference of a CCH-7 sample with its upper plate treated with polyimide is shown in figure 2 as a function of temperature. The sample thickness is 6·3 μm. As expected, the path difference decreases with increase in temperature, and

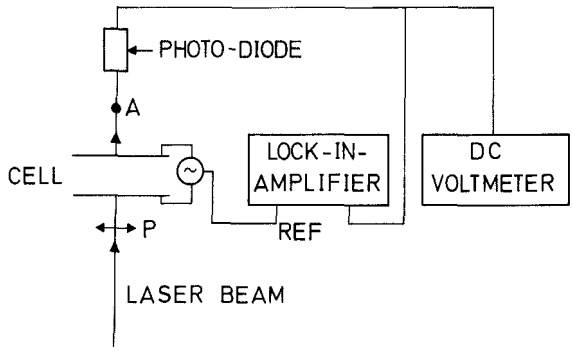

Figure 1. Block diagram of the experimental set up.

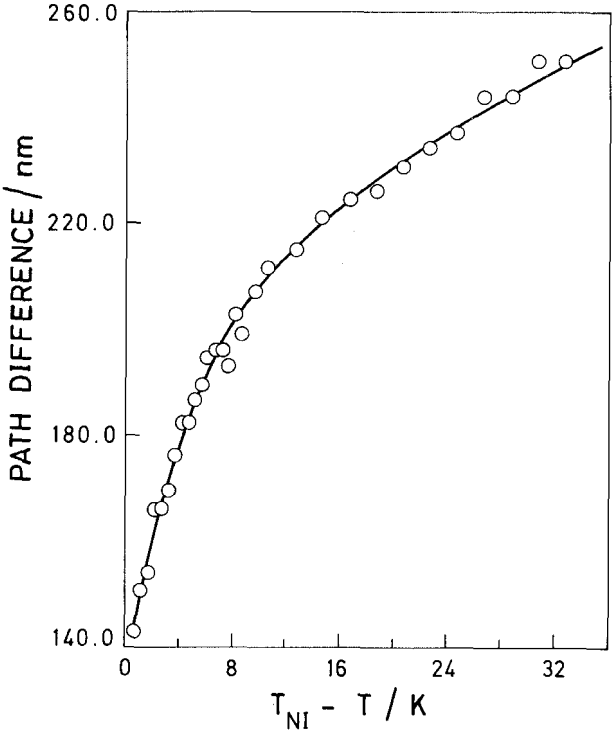

Figure 2. Variation of optical path difference (Δl) with temperature of CCH-7, cell thickness = 6·3 μm.

drops abruptly from a finite value to zero at the N–I transition. As we will show in the next section, the measured path difference indicates that the anchoring energy of the homeotropically aligned surface is relatively weak. We will also present the calculated temperature variation of the anchoring energy of the homeotropic surface in the next section.

We have also measured the electro-optic signals at $f = 23$ Hz on this cell at 60°C. The results are shown in figure 3. The DC signal continuously decreases as the applied voltage is increased. The f signal increases at first, but after attaining a maximum value, decreases, reaching a minimum, before it increases to a broad maximum (see figure 3). On the other hand, the $2f$ signal which is usually larger than the f signal rises to a broad maximum and then continuously decreases with the applied field. Similar results were found for an independent cell of greater thickness ($d \simeq 10\,\mu$m) (see figure 4).

In the case of PCH-7, the DC signal shows a maximum as a function of the applied field. At the same field, both f and $2f$ signals show minima. As the field increases, the f signal again shows a maximum and then a minimum, while the $2f$ signal shows a broad maximum (see figure 5).

3. Theoretical analysis and discussion

In the absence of the external field, the director profile is determined by the anchoring energies at the two surfaces and the elastic properties of the medium [1]. The director profile in the bulk is given by the elastic torque balance equation

$$(n \times h)^{\text{elastic}} = 0 \tag{1}$$

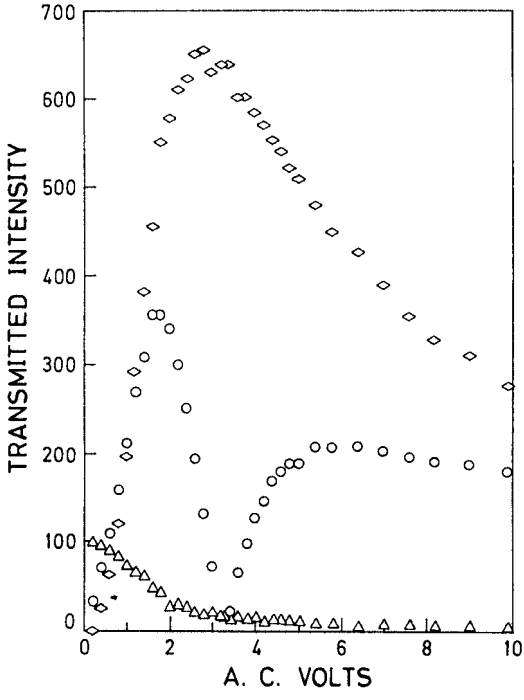

Figure 3. Electric field dependence of the DC (△), vertical scale in $\times 10^{-1}$ mV, f (○), vertical scale in μV and $2f$ (◇), vertical scale in μV, components of the optical signals. The sample is CCH-7 and the cell thickness 6·3 μm.

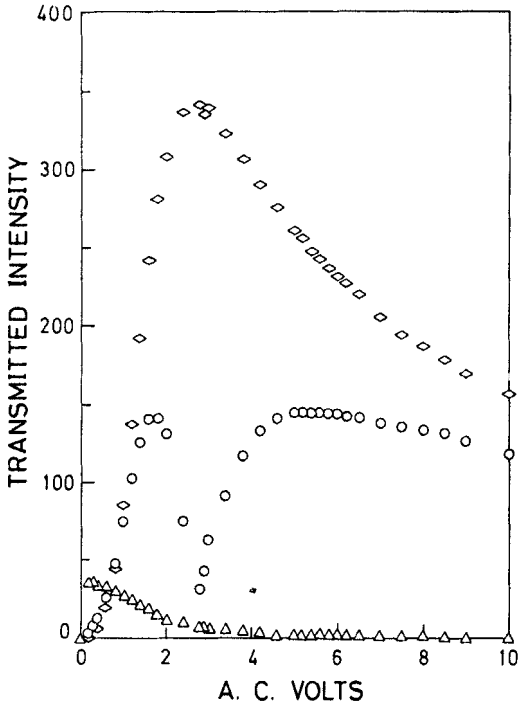

Figure 4. Electric field dependence of the DC (△), vertical scale in $\times 10^{-1}$ mV, f (○), vertical scale in μV, and 2 f (◇), vertical scale in μV, components of the optical signals in a CCH-7 sample of thickness 10 μm.

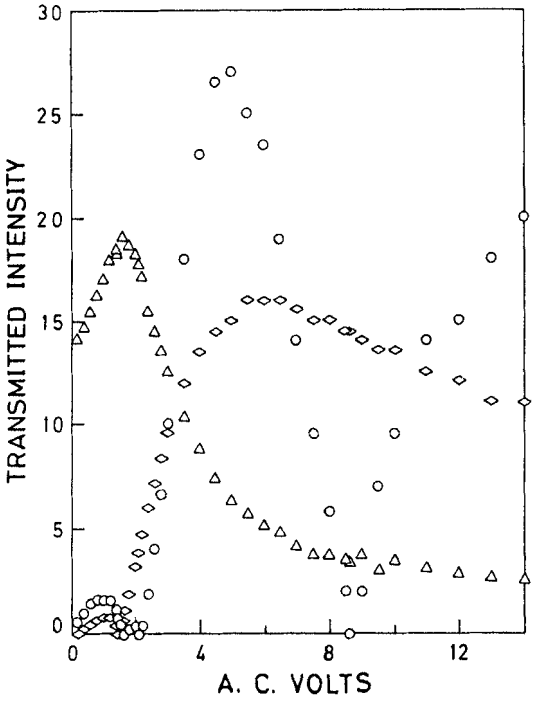

Figure 5. Electric field dependence of the DC (△), vertical scale in mV, f (○), vertical scale in 10^{-1} μv, and 2f (◇), vertical scale in μV, components of the optical signals in a PCH-7 sample of thickness 10·5 μm.

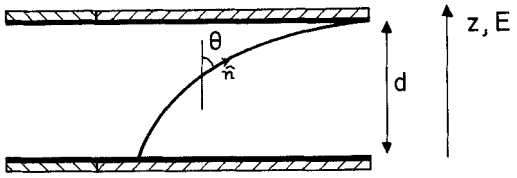

Figure 6. Schematic diagram of the director profile in a HAN cell.

where h is the relevant molecular field [1]. In the present problem (see figure 6) only the y-component of this equation is relevant and we get

$$(k_{11}\sin^2\theta + k_{33}\cos^2\theta)\frac{\partial^2\theta}{\partial z^2} + (k_{11}-k_{33})\sin\theta\cos\theta\left(\frac{\partial\theta}{\partial z}\right)^2 = 0, \tag{2}$$

where k_{11} and k_{33} are the splay and bend elastic constants, respectively. This equation can be easily integrated to obtain

$$z = \int_0^z dz = \frac{1}{c}\int_{\theta_{sl}}^{\theta} (k_{11}\sin^2\theta + k_{33}\cos^2\theta)^{1/2}\, d\theta, \tag{3}$$

where θ_{sl} is the tilt angle at the lower glass plate. $\theta(z)$ is the angle that the director makes with the z-axis and the constant of integration c is determined by the condition that the right hand side of equation (3) should integrate to yield d, the sample thickness, when the upper limit is θ_{su}, the tilt angle at the upper surface. θ_{sl} and θ_{su} are in turn determined by the surface torque balance conditions

$$W_l \sin\theta_{sl}\cos\theta_{sl} - (k_{11}\sin^2\theta_{sl} + k_{33}\cos^2\theta_{sl})\left(\frac{\partial\theta}{\partial z}\right)_{sl} = 0 \tag{4}$$

and

$$W_u \sin\theta_{su}\cos\theta_{su} - (k_{11}\sin^2\theta_{su} + k_{33}\cos^2\theta_{su})\left(\frac{\partial\theta}{\partial z}\right)_{su} = 0, \tag{5}$$

where W_l and the W_u are the anchoring energies at the lower and upper surfaces respectively.

We have measured the optical path difference of the hybrid aligned nematic cell (see figure 2). The path difference Δl is given by

$$\Delta l = \int_0^d (n_{eff}(z) - n_o)\, dz \tag{6}$$

where n_o is the ordinary index and the effective extraordinary refractive index, $n_{eff}(z)$ depends on $\theta(z)$

$$\frac{1}{n_{eff}^2(z)} = \frac{\cos^2\theta(z)}{n_o^2} + \frac{\sin^2\theta(z)}{n_e^2}, \tag{7}$$

where n_e is the principal extraordinary index of the medium. One can then write

$$\Delta l = n_o\left[\int_{\theta_{sl}}^{\theta_{su}} \frac{1}{c}\left(\frac{k_{11}\sin^2\theta + k_{33}\cos^2\theta}{1 - R\sin^2\theta}\right)^{1/2} d\theta - d\right], \tag{8}$$

where $R = (n_e^2 - n_o^2)/n_e^2$ and we have made use of the equation for $(d\theta/dz)$ arising from equation (2) to convert the z integration to a θ-integration. Our experiments have been

performed on CCH-7. The temperature dependence of the elastic constants and the refractive indices of CCH-7 have been obtained from [10] and [11] respectively. If we assume that both the surfaces have strong anchoring, i.e. $\theta_{sl}=0$ and $\theta_{su}=\pi/2$, the calculated value of the path difference is found to be smaller than that measured. This shows that $\theta_{sl}\neq 0$, i.e. the homeotropic anchoring is relatively weak. We now assume that the anchoring energy at the homogeneously aligned surface is strong and that $\theta_{su}=\pi/2$. Then, using equations (3), (4) and (8), we adjust the value of W_1 by an iterative numerical procedure so that the calculated value of Δl agrees with the experimental value. The resulting variation of W_1 with temperature is shown in figure 7. As the orientational order of the nematic decreases with temperature, the anchoring energy can also be expected to decrease, as is found in figure 7. We have also calculated the relevant extrapolation length $L=(k_{33}/W_1)$ whose temperature dependence is shown in figure 8. As expected, the extrapolation length is relatively high, $\sim 3\,\mu$m even at $T_{NI}-20°$. As the sample thickness $d=6{\cdot}2\,\mu$m, it is clear that the anchoring is indeed weak. Further, the extrapolation length increases to $\sim 4{\cdot}5\,\mu$m as the temperature is raised to T_{NI}. Such an increase has been noted earlier by Yokoyama *et al.* [12]. Their experiments were performed on 5CB oriented on an obliquely evaporated SiO surface, which gave rise to a much stronger anchoring ($L\sim 500$ Å far below T_{NI}). In view of the scatter in our data, we have not tried to fit these to any functional form.

As we have described in the experimental section, we have also measured the DC, f and $2f$ components of transmitted intensity as a function of an applied AC electric field. The f signal arises from oscillations of the θ-profile in the sample at the frequency

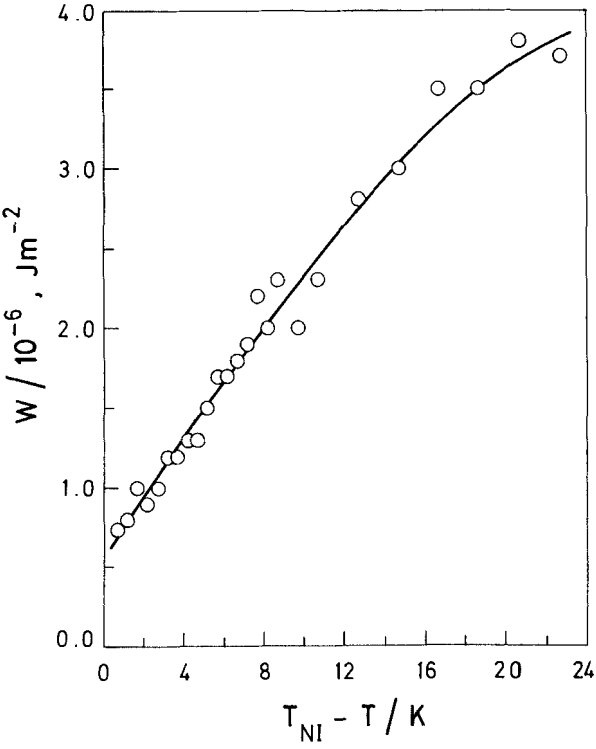

Figure 7. Temperature variation of the anchoring energy at the homeotropically aligned surface of the CCH-7 sample for which the optical data are given in figure 2.

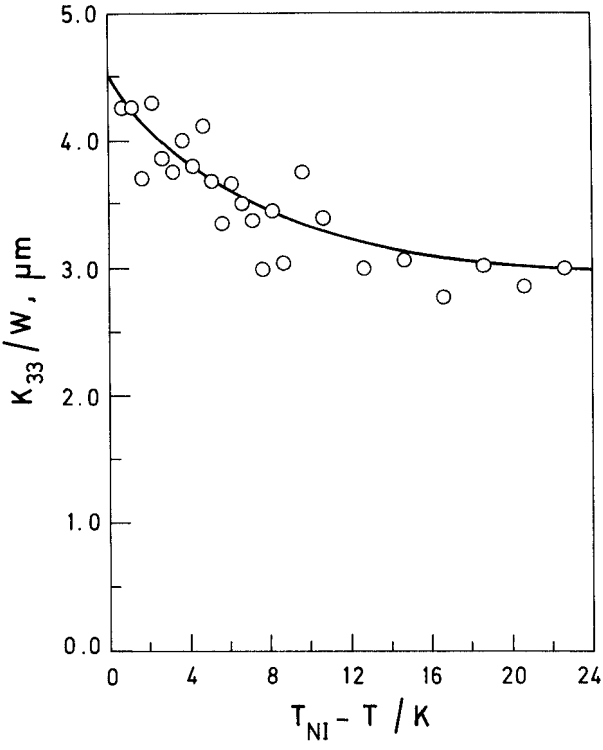

Figure 8. Temperature variation of the extrapolation length at the homeotropically aligned surface of the CCH-7 sample described in figure 2.

of the applied electric field. As we discussed earlier, the mechanism responsible for this oscillation is the flexoelectric effect which contributes to the surface torque, if the anchoring energy is weak. The $2f$ signal arises from the dielectric anisotropy of the medium, which is coupled quadratically with the field. Since the medium is viscous and the typical relaxation frequency of the director $\tau \sim \gamma d^2/k$ in the absence of the field is quite long, the amplitudes of these oscillations are rather small. The main effect of the field is the change in the director profile arising from the RMS voltage acting on the dielectric anisotropy, which rotates the director towards the field direction.

In CCH-7, the f signal increases initially as the voltage is increased, attains a maximum, and then decreases. It again increases after attaining a minimum value. The DC signal monotonically decreases with voltage. The $2f$ signal shows only a maximum. On the other hand, in PCH-7, both f and $2f$ signals go to zero at a voltage at which the DC signal shows a maximum. The f signal shows another minimum at a higher voltage. The first minimum shown by both f and $2f$ signals in PCH-7 can be attributed to an optical effect. In the geometry of the experiment, the transmission coefficient is given by

$$I = \frac{1 - \cos \Delta\phi}{2}, \tag{9}$$

where $\Delta\phi$ is the optical phase difference of the sample. If we now impose a small variation $\delta\Delta\phi$ in the phase difference, with $\delta\Delta\phi \ll 1$

$$I \simeq \tfrac{1}{2}\{1 - \cos \Delta\phi + \delta\Delta\phi \sin \Delta\phi\}, \tag{10}$$

i.e. the contribution from the additional phase difference vanishes for $\Delta\phi = n\pi$, where n is an integer. As can be seen from equation (9), $n = 1$ gives rise to the maximum in the DC signal and a vanishing of both f and $2f$ signals. This corresponds to the first minimum in PCH-7. However, the second minimum in the f signal in this case and the minimum in CCH-7 require a different explanation. We have already noted that the f signal arises from the flexoelectric contribution to the surface torque. In CCH-7, our earlier experiment has shown that the homeotropically aligned surface has a relatively weak anchoring so that θ_{sl} has a non-zero value even in the absence of the external field. This gives rise to the f signal at low fields, which increases with the applied field. However, as the field is increased further, the dielectric torque on the medium, depending quadratically on the field, reduces the value of θ_{sl}, thus reducing the flexoelectric signal. At even higher fields, the dielectric torque is sufficient to affect the tilt angle θ_{su} at the homogeneously aligned surface which has a relatively strong anchoring. This in turn gives rise to a flexoelectric torque on that surface, and hence an increase in the f signal. This would explain our observation of the minimum in the f signal. On the other hand, the $2f$ signal depends on the dielectric contribution in the bulk. The signal initially increases, but as the average director profile approaches one of uniform orientation along the field direction at high fields, the $2f$ signal gradually decreases. The field variation of the f signal can in principle be used to measure the anchoring energies at the two surfaces. In order to bring out this possibility, we now give a highly simplified theoretical model, reserving a more detailed analysis to a later publication. We make the one elastic constant approximation, i.e. we assume $k_{11} = k_{33} = K$. The dielectric anisotropy produces a non-uniform electric field distribution in the cell which is ignored in the present analysis. As the director orientation is time dependent, we have to take into account the dissipative contribution to the torque. We again simplify, ignoring the contribution due to backflow. With these simplifications, the torque balance equation in the bulk is given by

$$\gamma_1 \dot{\theta} - K\frac{\partial^2\theta}{\partial z^2} + \frac{\Delta\varepsilon E^2 \sin 2\theta}{8\pi} = 0, \tag{11}$$

where γ_1 is the rotational viscosity coefficient, $\Delta\varepsilon$ the dielectric anisotropy and $E = E_0 \sin \omega t$ is the applied AC field. The boundary conditions are

$$\frac{W \sin 2\theta_s}{2} - K\left(\frac{\partial\theta}{\partial z}\right)_s - \frac{(e_1 + e_3)E \sin 2\theta_s}{2} = 0, \tag{12}$$

where s stands for either surface, and $(e_1 + e_3)$ is the sum of the flexoelectric coefficients. As the f and $2f$ signals are very small, it is clear that the time dependent part of θ has a very small amplitude. Writing

$$\theta(z) = \theta_0(z) + \theta_t(z) \tag{13}$$

where the subscript t indicates time dependence, we expand the θ-dependent function in equations (11, 12) to the first power in θ_t. The time independent part of equation (11) reads

$$-K\frac{\partial^2\theta_0}{\partial z^2} + \frac{\Delta\varepsilon E_0^2 \sin 2\theta_0}{8\pi} = 0, \tag{14}$$

with the corresponding boundary conditions

$$\frac{W\sin 2\theta_{0s}}{2}-K\left(\frac{\partial\theta_0}{\partial z}\right)_s=0. \tag{15}$$

In the present paper, we will only analyse the part of $\theta_t(z)$ which oscillates at f, the frequency of the applied AC field, ignoring the $2f$ component. In general, we can write

$$\theta_t(z)=\theta_1(z)\sin\omega t+\theta_2(z)\cos\omega t. \tag{16}$$

The corresponding torque balance equations in the bulk are

$$\gamma\omega\theta_2+K\frac{\partial^2\theta_1}{\partial z^2}=0 \tag{17a}$$

and

$$\gamma_1\omega\theta_1-K\frac{\partial^2\theta_2}{\partial z^2}=0. \tag{17b}$$

The boundary conditions are

$$W\cos 2\theta_{0s}\theta_{1s}-K\left(\frac{\partial\theta_1}{\partial z}\right)_s-\frac{(e_1+e_3)E_0}{2}\sin 2\theta_{0s}=0 \tag{18}$$

and

$$W\cos 2\theta_{0s}\theta_{2s}-K\left(\frac{\partial\theta_2}{\partial z}\right)_s=0, \tag{19}$$

where, as before, s stands for either boundary. (17 *a*) and (17 *b*) can be solved to obtain

$$\theta_1(z)=c_1\sin bz\sinh bz+c_2\cos bz\cosh bz+c_3\cos bz\sinh bz+c_4\sin bz\cosh bz, \tag{20}$$

where c_1 to c_4 are constants and

$$b=\left(\frac{\gamma_1\omega}{2K}\right)^{1/2}. \tag{21}$$

The amplitude $\theta_2(z)$ reads as

$$\theta_2(z)=c_2\sin bz\sinh bz+c_3\sin bz\cosh bz-c_4\cos bz\sinh bz-c_1\cos bz\cosh bz. \tag{22}$$

Using the four boundary conditions given by equations (18) and (19) at $z=0$ and d, we calculate the coefficients c_1 to c_4. In the calculations, we first integrate equation (14) to obtain

$$z=\int_0^z dz=\int_{\theta_{0s1}}^{\theta_0}\frac{d\theta_0}{\left(G+\dfrac{\Delta\varepsilon E_0^2}{8\pi K}\sin^2\theta_0\right)^{1/2}}, \tag{23}$$

where G is a constant of integration which is chosen such that when $z=d$, $\theta_0=\theta_{0su}$, the tilt angle at the upper plate. θ_{0su} and θ_{0sl} in turn should satisfy the boundary conditions (15) at the upper and lower plates respectively, with the corresponding anchoring strengths taken as W_u and W_l. In the calculations, we assume some values of W_l and W_u such that $W_l<W_u$ and numerically calculate θ_{0sl}, θ_{0su} and G iteratively to satisfy the above equations.

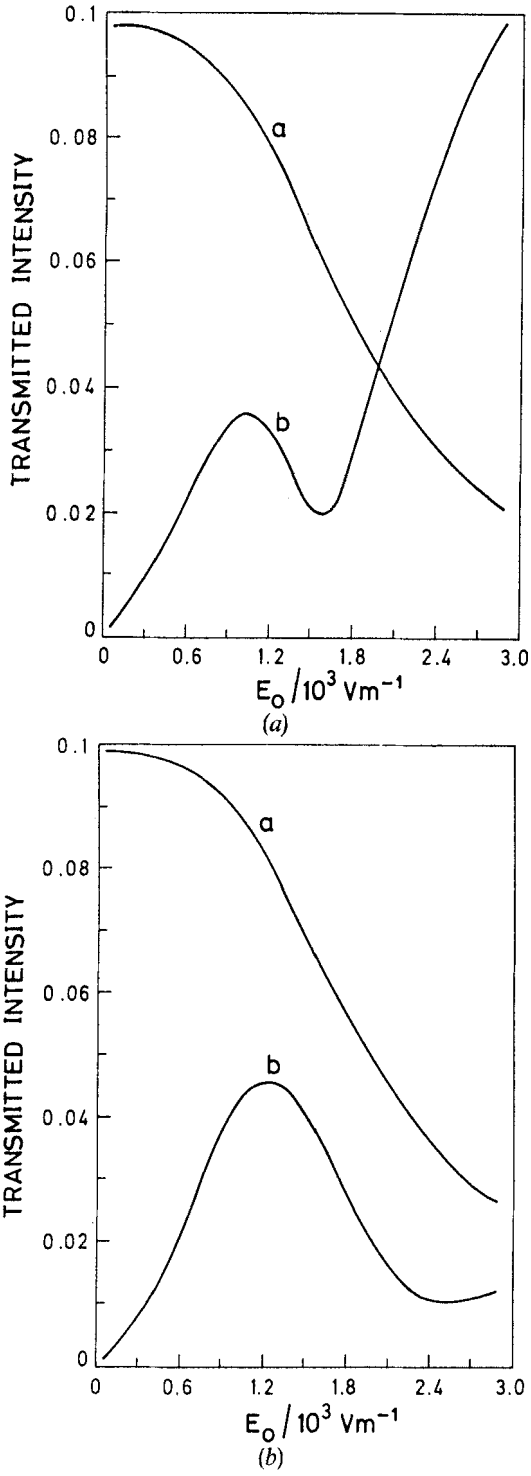

Figure 9. Calculated field dependence of the DC (line a), vertical scale $\times 10^{-1}$ in arbitrary units and f (line b) optical signals with $d = 10\,\mu m$, $f = 11$ Hz and the CCH-7 material parameters. (*a*) $W_l = 5 \times 10^{-6}\,J\,m^{-2}$, $W_u = 2 \times 10^{-5}\,J\,m^{-2}$ and (*b*) $W_l = 5 \times 10^{-6}\,J\,m^{-2}$, $W_u = 6 \times 10^{-5}\,J\,m^{-2}$. Horizontal scale $\times 10^{-2}$.

The transmitted intensity is given by equation (9) in which the phase difference $\Delta\phi = 2\pi\Delta l/\lambda$, where Δl is the path difference, given by equation (6). The DC signal I_0 which is the time-independent part of the intensity is calculated using the equation

$$\Delta l_0 = n_0 \left[\int_{\theta_{0sl}}^{\theta_{0su}} \frac{d\theta_0}{\left[(1 - R\sin^2\theta_0)\left(G + \frac{\Delta\varepsilon E_0^2}{8\pi K}\sin^2\theta_0 \right) \right]^{1/2}} - d \right]. \tag{24}$$

The in-phase component of the transmitted intensity at the frequency f of the applied field is calculated using the $\delta\Delta\phi$ part of equation (10), which is equal to $(2\pi/\lambda)\Delta l_1$, where

$$\Delta l_1 = \frac{n_0}{2} \int_{\theta_{0sl}}^{\theta_{0su}} \frac{\sin 2\theta_0(z)}{(1 - R\sin^2\theta_0)^{3/2}} \frac{\theta_1(z)\, d\theta_0}{\left(G + \frac{\Delta\varepsilon E_0^2}{8\pi K}\sin^2\theta_0 \right)^{1/2}}. \tag{25}$$

In the above equation, note that the integration is performed over θ_0 as $\theta_1(z)$ is an implicit function of θ_0. We use Simpson's rule with 41 intervals in between θ_{0sl} and θ_{0su} in our calculations. Using equation (23), we determine the values of z at the values of θ_0 needed in later calculations. The path difference corresponding to the out of phase oscillations, viz. Δl_2, is given by an expression similar to (25) obtained by replacing θ_1 by θ_2.

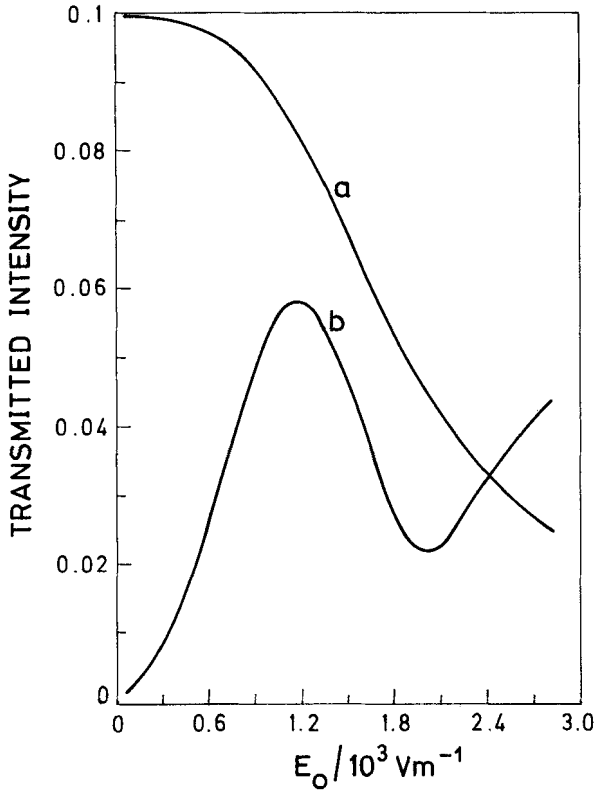

Figure 10. Calculated field dependence of the DC (line a), vertical scale $\times 10^{-1}$ in arbitrary units and f (line b) optical signals with $d = 10\,\mu m$, f = 11 Hz and $W_l = 4 \times 10^{-6}\,J\,m^{-2}$ and $W_u = 3 \times 10^{-5}\,J\,m^{-2}$ for CCH-7. Horizontal scale $\times 10^{-2}$.

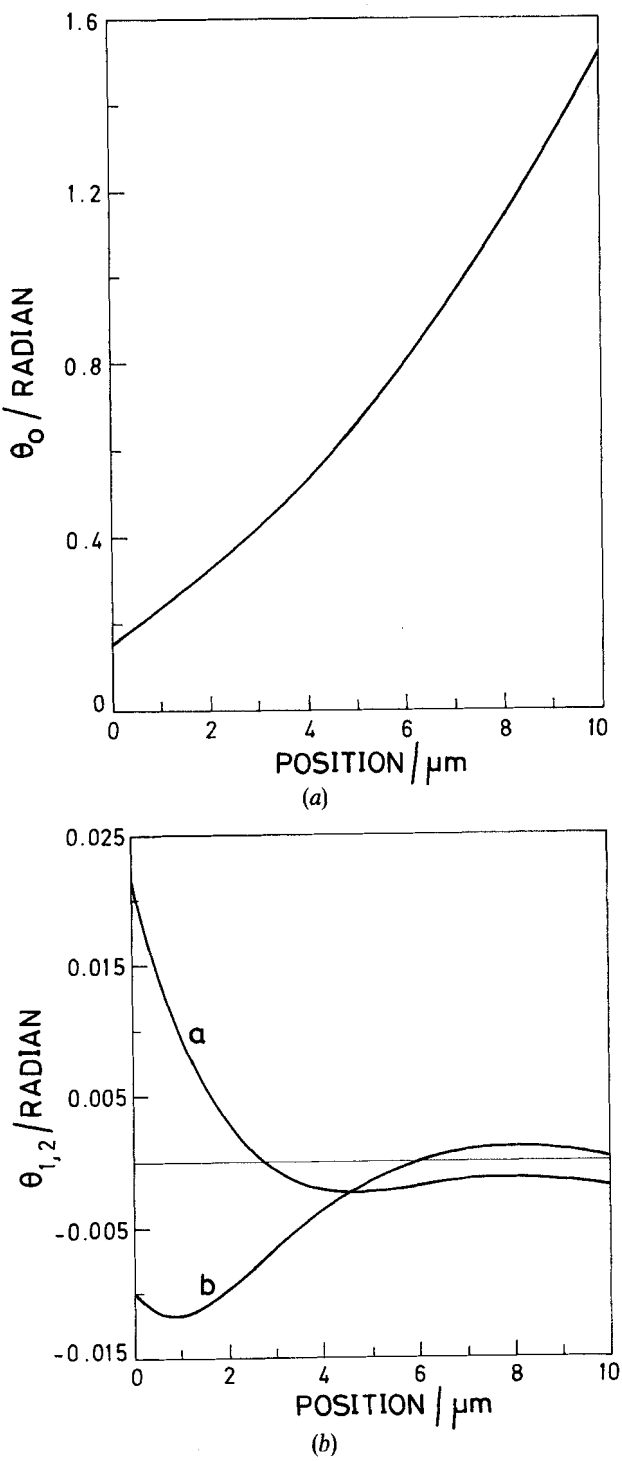

Figure 11. Calculated z-variation of (*a*) θ_0 and (*b*) θ_1 (line a) and θ_2 (line b). The sample CCH-7, the cell thickness 6·3 μm and $E_0 = 12 \times 10^4$ V m^{-1}.

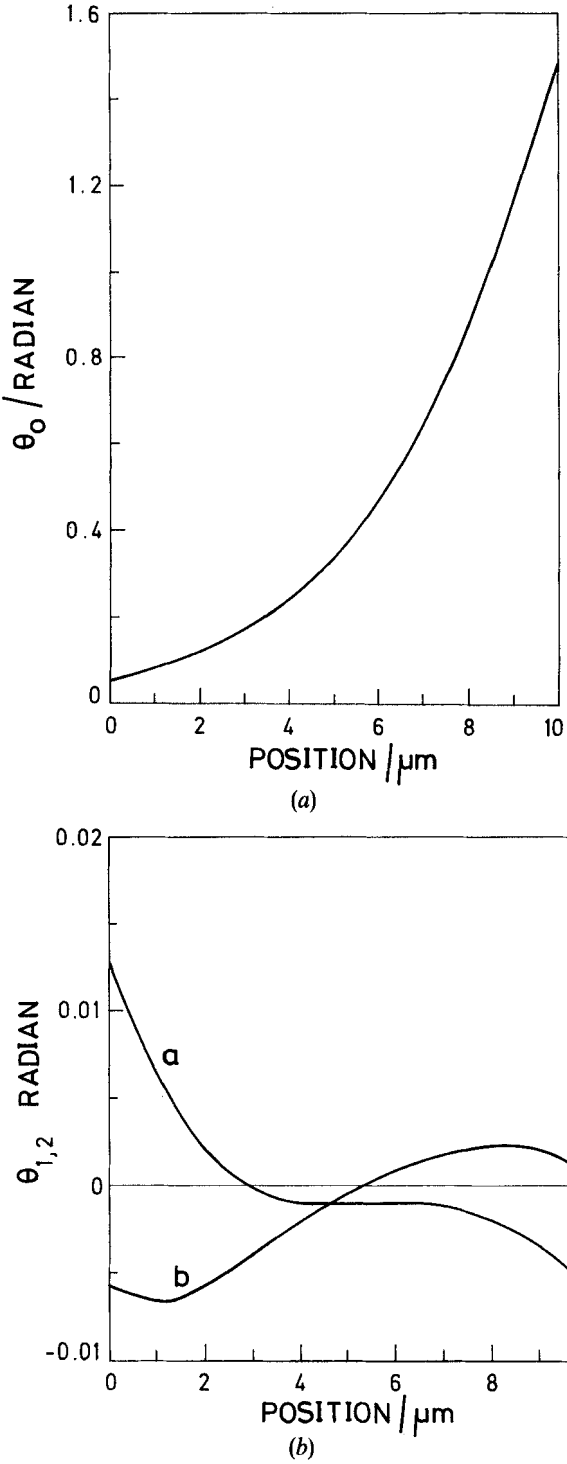

Figure 12. Calculated z-variation of (*a*) θ_0 and (*b*) θ (line a) and θ_2 (line b). $E_0 = 21{\cdot}6 \times 10^4\ \mathrm{V\,m^{-1}}$.

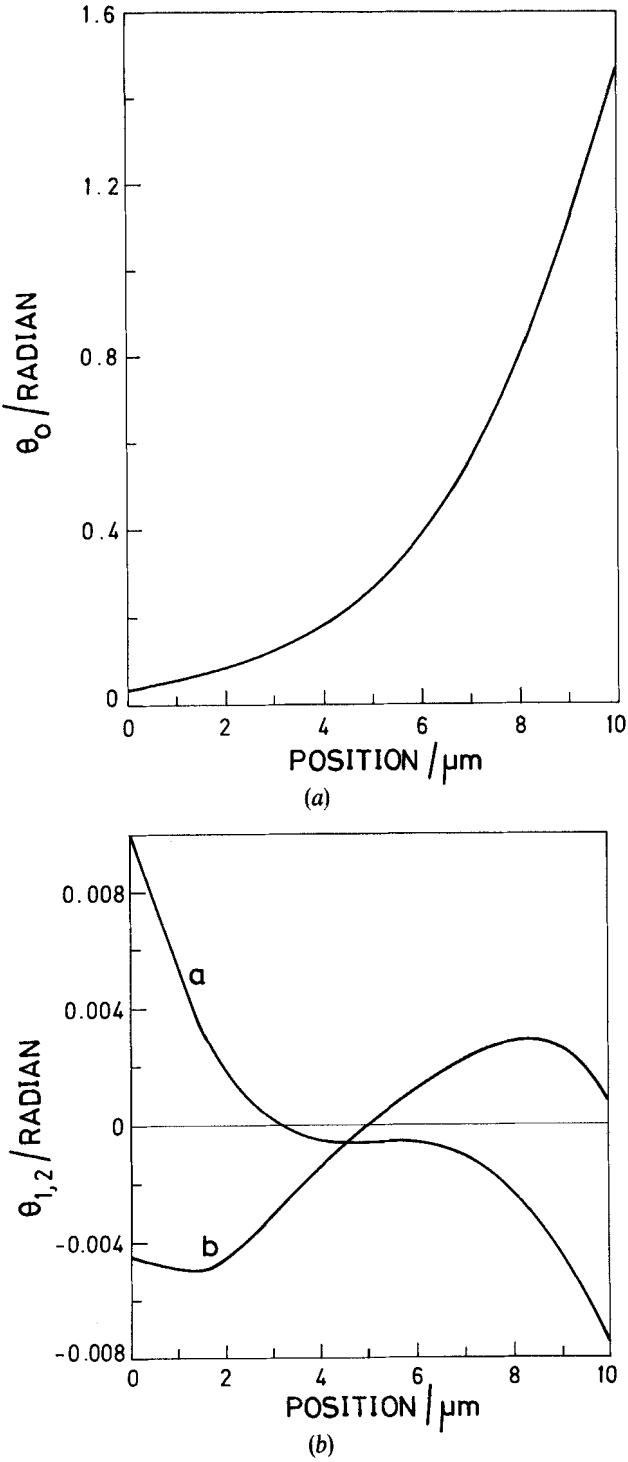

Figure 13. Calculated z-variation of (*a*) θ_0 and (*b*) θ (line a) and θ_2 (line b). $E_0 = 24{\cdot}6 \times 10^4\,\mathrm{V\,m^{-1}}$.

Calculations were performed for material parameters similar to those of both CCH-7 and PCH-7. For CCH-7 we took $K = 8 \times 10^{-12}$ N, $\gamma_1 = 0{\cdot}04$ Ns m^{-2}, $n_e = 1{\cdot}5055$, $n_o = 1{\cdot}4531$ and $\Delta\varepsilon = 4{\cdot}1$ [10, 11]. For PCH-7, the assumed values are: $K = 13{\cdot}1 \times 10^{-12}$ N, $\gamma_1 = 0{\cdot}05$ Ns m^{-2}, $n_e = 1{\cdot}5960$, $n_o = 1{\cdot}4782$ and $\Delta\varepsilon = 10{\cdot}25$ [13, 14].

As the field is increased to very high values, the director is practically along the z-axis in most of the sample and the variations in θ occur over a very narrow thickness close to the homogeneously aligned surface. The accuracy of our present calculations is not adequate to cover such high fields.

Figures 9 (*a*) and (*b*) show the influence on the optical signals on W_u, the anchoring energy at the homogeneously aligned surface with a fixed value of W_l which corresponds to the homeotropically aligned surface, for CCH-7 parameters. Using $f = 11$ Hz and $W_l = 5 \times 10^{-6}$ J m^{-2}, figure 9 (*a*) gives the results for $W_u = 2 \times 10^{-5}$ J m^{-2} and figure 9 (*b*) for $W_u = 6 \times 10^{-5}$ J m^{-2}. It is clear that the minimum in the f signal shifts towards higher fields for higher values of W_u, as may be expected. The DC signal decreases monotonically with increase of the field in conformity with the experimental result. Figure 10 shows the DC and f signals for $W_l = 4 \times 10^{-6}$ J m^{-2}, $W_u = 3 \times 10^{-5}$ J m^{-2}, $d = 10\,\mu$m and $f = 11$ Hz. The ratio of f signal to DC signal at the maximum of the former agrees with the experimental curve shown in figure 4. In order to bring out the mechanism for the occurrence of the minimum in the f signal, we have plotted, θ_0, θ_1 and θ_2 as functions of z at different values of the applied field in figures 11

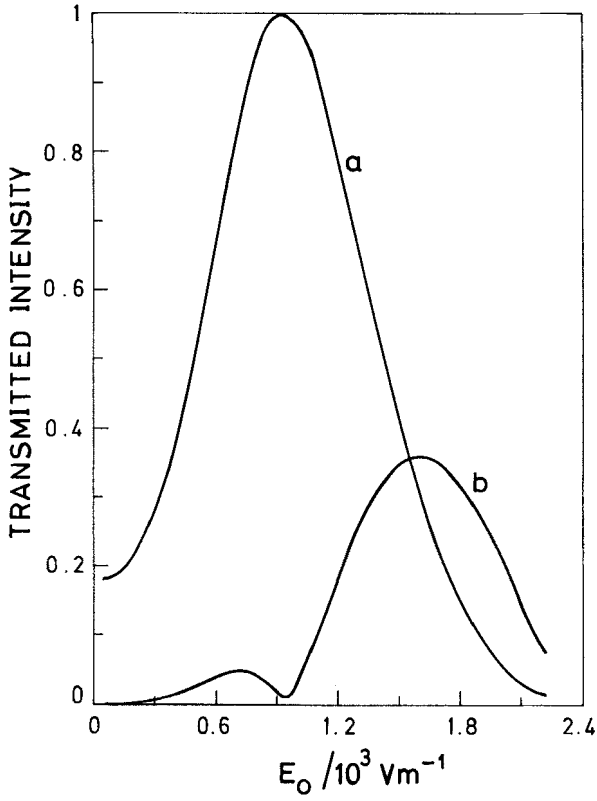

Figure 14. Calculated field dependence of the DC (line a), vertical scale $\times 10^{-1}$ in arbitrary units and f (line b), optical signals. $d = 9{\cdot}9\,\mu$m, $f = 23$ Hz and the PCH-7 parameters are $W_l = 6{\cdot}3 \times 10^{-6}$ J m^{-2}, $W_u = 6 \times 10^{-6}$ J m^{-2}. Horizontal scale $\times 10^{-2}$.

to 13. At low fields, the homeotropically aligned surface which has the lower anchoring is characterized by a value of θ_{0sl} which is considerably different from 0 (see figure 11 (*a*)). Consequently, the amplitudes θ_1 and θ_2 take very high values close to this surface (see figure 11 (*b*)). As the field is increased, and θ_{0sl} at this plate becomes smaller (see figure 12 (*a*)), the flexoelectric surface torque ($\propto \sin 2\theta_{0s}$) decreases and the amplitudes θ_1 and θ_2 also decrease (see figure 12 (*b*)) giving rise to a decrease in the *f* signal. At even higher fields, the surface tilt angle at the homogeneously aligned plate decreases significantly from $\pi/2$ (see figure 13 (*a*)) and as the curvature is now confined to a small thickness close to this plate, the effective anchoring energy becomes weaker. Hence the amplitudes θ_1 and θ_2 increase at this plate (see figure 13 (*b*)), and the *f* signal again increases.

Figure 14 illustrates the calculations based on the material parameters of PCH-7. In this case, the homogenous alignment was obtained by an oblique SiO coating. We had to assume that the anchoring energies at the two surfaces have similar values to reproduce the experimental trends. The DC signal shows a maximum as a function of the field. As discussed earlier (see equation (9)), the AC signal itself goes to zero at the same value of the field. We have not been able to extend the calculations to high enough fields to get the second minimum in the *f* signal in this case. However, the present analysis clearly emphasizes that an oblique coating of SiO does not yield a high

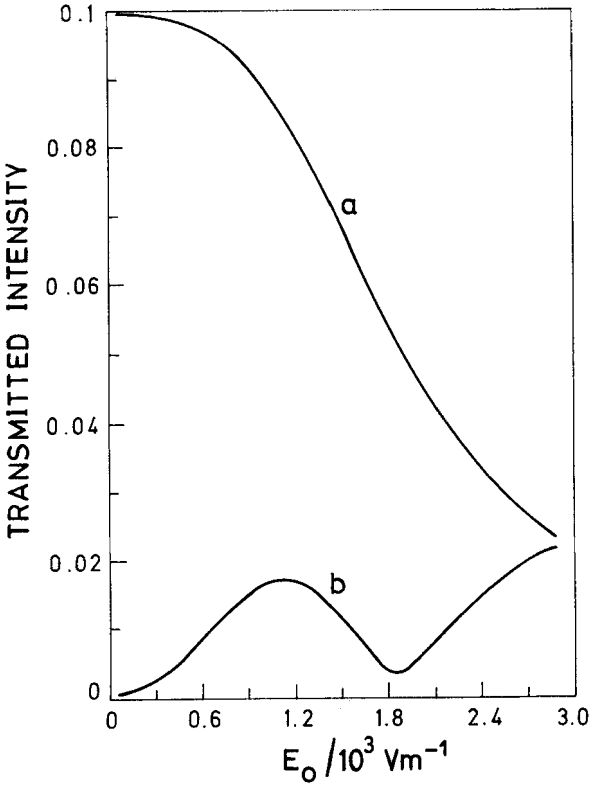

Figure 15. Calculated field dependence of the DC (line a), vertical scale $\times 10^{-1}$ in arbitrary units, and *f* (line b) optical signals where $d = 10\,\mu$m $f = 33$ Hz and $W_l = 4 \times 10^{-6}$ J m^{-2} and $W_u = 3 \times 10^{-5}$ J m^{-2} for CCH-7. Horizontal scale $\times 10^{-2}$.

anchoring energy for PCH-7, possibly because of the predominance of aliphatic groups in the molecule.

Our present model is oversimplified and simply illustrates the potential of this technique. A rigorous theory can be used to measure both W_l and W_u. The ratio of the f signal at its maximum to the DC signal at the same field depends on both W_l and W_u and on (e_1+e_3). Clearly if (e_1+e_3) increases, the f signal should increase. Further, if we increase the frequency (figure 15 compared to figure 10), the maximum value of the f signal decreases. These data could be used to measure not only W_l, W_u and (e_1+e_3) but also γ_1. The minimum in the f signal depends on W_u/W_l and could be used to measure that ratio. We are now developing a rigorous theoretical model to use this technique for calculating all these parameters from the experimental data.

References

[1] De Gennes, P. G., 1975, *The Physics of Liquid Crystals* (Clarendon).
[2] Rosenblatt, C., 1984, *J. Phys., Paris*, **45**, 1087.
[3] Yokoyama, H., and Van Sprang, H. A., 1985, *J. appl. Phys.*, **57**, 4520.
[4] Blinov, L. M., Sonin, A. A., and Barnik, M. I., 1989, *Sov. Phys. Crystallogr.*, **34**, 245.
[5] Barbero, G., Madhusudana, N. V., and Durand, G., 1984, *J. Phys. Lett., Paris*, **45**, L-613.
[6] Ryshenkov, G., and Kleman, M., 1976, *J. chem. Phys.*, **64**, 404.
[7] Riviere, D., Levy, Y., and Guyon, E., 1979, *J. Phys. Lett., Paris*, **40**, 215.
[8] Barbero, G., and Barberi, R., 1983, *J. Phys., Paris*, **44**, 609.
[9] Madhusudana, N. V., and Durand, G., 1985, *J. Phys. Lett., Paris*, **46**, L-195.
[10] Schad, Hp., and Osman, M. A., 1981, *J. chem. Phys.*, **75**, 880.
[11] Pohl, L., Eidenschink, R., Krause, J., and Weber, G., 1978, *Phys. Lett.*, **65A**, 169.
[12] Yokoyama, H., Kobayashi, S., and Kamei, H., 1987, *J. appl. Phys.*, **61**, 4501.
[13] Schad, Hp., Baur, G., and Meier, G., 1979, *J. chem. Phys.*, **70**, 2770.
[14] Sen, S., Kali, K., Roy, S. K., and Roy, S. B., 1985, *Molec. Crystals liq. Crystals*, **126**, 269.